Journal of Solid State Chemistry **145,** 283–290 (1999)
Article ID jssc.1999.8265, available online at http://www.idealibrary.com on IDEAL®

Structure and Properties of $Sr_2Au_3In_4$ and $Eu_2Au_3In_4$

Rolf-Dieter Hoffmann,* Rainer Pöttgen,* Carsten Rosenhahn,† Bernd D. Mosel,† Bernd Künnen,* and Gunter Kotzyba*

*Anorganisch-Chemisches Institut, Universität Münster, Wilhelm-Klemm-Strasse 8, D-48149 Münster, Germany; and †Institut für Physikalische Chemie, Universität Münster, Schlossplatz 4/7, D-48149 Münster, Germany
E-mail: pottgen@uni-muenster.de; mosel@uni-muenster.de

Received November 25, 1998; in revised form February 24, 1999; accepted March 10, 1999

$Sr_2Au_3In_4$ was synthesized by reacting the elements in glassy carbon crucibles under an argon atmosphere in a high-frequency furnace. $Eu_2Au_3In_4$ was obtained in the same way but starting with EuAuIn as a precursor and admixing indium and gold. Both compounds were investigated by X-ray diffraction on powders and single crystals: anti-$Hf_2Co_4P_3$ type, $P\bar{6}2m$, $a = 1501.6(9)$ pm, $c = 457.9(2)$ pm, w$R2 = 0.0734$, 1030 F^2 values, 45 variables for $Sr_2Au_{2.85}In_{4.15}$ and $a = 1489.7(3)$ pm, $c = 454.90(7)$ pm, w$R2 = 0.1222$, 1051 F^2 values, 45 variables for $Eu_2Au_3In_4$. One gold site in the strontium compound shows a mixed occupancy with indium atoms indicating a small homogeneity range according to $Sr_2Au_{3-x}In_{4+x}$. Striking structural motifs of $Sr_2Au_3In_4$ and $Eu_2Au_3In_4$ are gold-centered trigonal prisms formed by the strontium (europium) and indium atoms. All gold atoms have coordination number 9 in the form of tricapped trigonal prisms. The indium atoms in $Sr_2Au_3In_4$ and $Eu_2Au_3In_4$ occupy the cobalt positions of the $Hf_2Co_4P_3$ type and the more electronegative gold atoms take the phosphorus positions, indicating that $Sr_2Au_3In_4$ and $Eu_2Au_3In_4$ may be considered as ternary aurides. The gold and indium atoms form three-dimensional $[Au_3In_4]^{4-}$ polyanions in which the divalent strontium and europium atoms occupy distorted hexagonal tubes. Magnetic susceptibility measurements of $Eu_2Au_3In_4$ show paramagnetic behavior above 50 K with an experimental magnetic moment of 7.88(5) μ_B/Eu indicating Eu^{2+}. Antiferromagnetic ordering is detected at 9.5(5) K at low external fields. A metamagnetic transition is observed at 2 K at a critical field of 0.5(2) T. The experimental saturation moment at 2 K and 5.5 T is 5.95(5) μ_B/Eu. Electrical conductivity investigations exhibit metallic behavior with a room temperature value of 75 ± 10 μΩcm for the specific resistivity. ^{151}Eu Mössbauer spectroscopic measurements show a broadened line with an isomer shift of $-10.5(5)$ mm/s at 78 K in accordance with several sites of divalent europium. Below 10 K magnetic hyperfine field splitting is observed. © 1999 Academic Press

Key Words: **intermetallic compounds; crystal structure; antiferromagnetism; ^{151}Eu Mössbauer spectroscopy.**

INTRODUCTION

The ternary systems rare earth metal–transition metal–indium have intensively been investigated in recent years (1). These investigations resulted in numerous new intermetallic compounds with a variety of different crystal structures (2) and interesting magnetic and electrical properties (3). When it comes to the structural characterization of the respective systems with europium, ytterbium, or the alkaline earth elements as electropositive components, only very few systems have been studied. Detailed phase analytical investigations have only been performed in the systems Ca–Cu–In (4, 5) and Eu–Ag–In (6). Very recent investigations of other ternary systems led to the syntheses of a variety of new ternary compounds with divalent cations, i.e., CaTIn (T = Rh, Pd, Pt, Au) (7–9), $CaTIn_2$ (T = Ni, Cu, Pd, Pt, Au) (4, 10, 11), $SrTIn_2$ (T = Rh, Pd, Ir, Pt) (12), $CaAg_2In_4$ and $YbAg_2In_4$ (13), $EuNiIn_2$ (14), $EuPdIn_2$, $YbPdIn_2$, and $YbAuIn_2$ (15), $EuCuIn_4$ (4), $EuNiIn_4$, and $YbNiIn_4$ (16, 17).

Herein we report on the new indium compounds $Sr_2Au_3In_4$ and $Eu_2Au_3In_4$ which are isotypic with $Hf_2Co_4P_3$ (18). Besides the equiatomic compounds like CaAuIn (8) with TiNiSi type structure, $Sr_2Au_3In_4$ and $Eu_2Au_3In_4$ are the first examples for indium compounds which adopt a typical structure of a metal-rich phosphide where the phosphorus sites are occupied by the partially negatively charged gold atoms.

EXPERIMENTAL

Starting materials for the preparation of $Sr_2Au_3In_4$ and $Eu_2Au_3In_4$ were ingots of strontium and europium (Johnson Matthey, $-$ 99.9%), gold wire (Degussa, ∅ 1 mm, $>$ 99.9%), and indium tear drops (Johnson Matthey, $>$ 99.9%). Two slightly different routes were employed for the syntheses of these compounds. To obtain single phase

0022-4596/99 $30.00

products the nominal composition needed to be in the ideal atomic ratio of (Sr, Eu):Au:In = 2:3:4 for each synthesis.

$Sr_2Au_3In_4$ was prepared by high-frequency melting (Hüttinger Elektronik, Freiburg, Typ TIG 1.5/300) of the elements in the ideal 2:3:4 atomic ratio as well as with the atomic ratio 2:2:4 in a glassy carbon crucible (Sigradur®G, glassy carbon, type GAZ006) under flowing argon. The argon was purified over silica gel, molecular sieves, and titanium sponge (900 K). The glassy carbon crucibles were placed in a water-cooled sample chamber made of Duran® glass as described in detail in Ref. (8). During the inductive heating process, the gold wire and the indium drops first form an alloy at low temperature which finally reacts with the strontium pieces in a strongly exothermic reaction. No weight loss was observed after the reaction. After cooling down to room temperature, the sample could easily be separated from the glassy carbon crucible by pounding at its base. No reactions of the sample with the crucible could be detected. The crystal for the single crystal X-ray investigation was taken from a sample with a lower gold content (Sr:Au:In = 2:2:4) as the ideal formula requires. For this crystal the refined composition was $Sr_2Au_{2.85}In_{4.15}$ in accordance with energy dispersive X-ray analyses of the polished sample (initial composition 2:2:4). The analyses were carried out with a scanning electron microscope in backscattering mode. The range of homogeneity was not investigated any further.

$Eu_2Au_3In_4$ was prepared by the same method, however, starting with a sample of equiatomic EuAuIn as a precursor which was synthesized in a tantalum tube (19). The brittle sample of EuAuIn was first ground to a coarse-grained powder and then mixed with the appropriate amounts of gold wire and indium tear drops. The reaction of these three components was far less exothermic as compared to the reaction of elemental strontium with gold and indium for the synthesis of $Sr_2Au_3In_4$. The resulting button of $Eu_2Au_3In_4$ could easily be separated from the glassy carbon crucible. No impurity phases could be detected on the Guinier powder pattern.

$Sr_2Au_3In_4$ and $Eu_2Au_3In_4$ are stable against air and moisture in the form of compact buttons as well as fine-grained powders. No decomposition was observed after several weeks. Single crystals of these compounds exhibit metallic luster.

Guinier powder patterns of the samples were recorded with Cu$K\alpha_1$ radiation using α-quartz ($a = 491.30$ pm, $c = 540.46$ pm) as an internal standard. The hexagonal lattice constants (see Table 1) were obtained from least-squares fits of the Guinier data. To assure correct indexing, the observed patterns were compared with calculated ones (20) taking the atomic positions from the structure refinements. In the case of $Sr_2Au_3In_4$ the homogeneity range was clearly visible by line shifts on the powder patters of samples with the nominal compositions Sr:Au:In = 2:2:4 and 2:3:4. The variations of the lattice constants were: $a = 1501.6(9)$, $c = 457.9(2)$ pm, $V = 0.8941$ nm^3 for an initial composition of Sr:Au:In = 2:2:4 and $a = 1498.0(3)$, $c = 456.09(7)$ pm, $V = 0.8863$ nm^3 for Sr:Au:In = 2:3:4. Thus, the indium rich sample shows larger lattice constants as can be expected comparing Pauling's single bond radii of gold (133.6 pm) and indium (149.7 pm) (21).

TABLE 1
Crystal Data and Structure Refinement for the Hexagonal Compounds $Sr_2Au_{2.85}In_{4.15}$ and $Eu_2Au_3In_4$ ($Z = 4$, space group $P\bar{6}2m$, No. 189)

Empirical formula	$Sr_2Au_{2.85}In_{4.15}$	$Eu_2Au_3In_4$
Formula weight	1213.10 g/mol	1354.10 g/mol
Lattice constants	$a = 1501.6(9)$ pm	$a = 1489.7(3)$ pm
(Guinier powder data)	$c = 457.9(2)$ pm	$c = 454.90(7)$ pm
	$V = 0.8941$ nm^3	$V = 0.8743$ nm^3
Calculated density	9.01 g/cm^3	10.29 g/cm^3
Crystal size	$12 \times 12 \times 60$ μm^3	$30 \times 25 \times 15$ μm^3
Transmission (max/min)	1.49	2.26
Absorption coefficient	68.8 mm^{-1}	74.5 mm^{-1}
$F(000)$	2018	2236
θ range for data collection	2° to 30°	2° to 32°
Scan type	$\omega/2\theta$	$\omega/2\theta$
Range in hkl	$\pm 21, \pm 21, \pm 6$	$\pm 22, \pm 22, \pm 6$
Total no. reflections	7520	6060
Independent reflections	1030 ($R_{int} = 0.1446$)	1051 ($R_{int} = 0.1625$)
Reflections with $I > 2\sigma(I)$	734 ($R_{sigma} = 0.0670$)	688 ($R_{sigma} = 0.0874$)
Data/restraints/parameters	1030/0/45	1051/0/45
Goodness-of-fit on F^2	1.116	1.107
Final R indices [$I > 2\sigma(I)$]	$R1 = 0.0311$	$R1 = 0.0481$
R indices (all data)	$R1 = 0.0782$	$R1 = 0.1021$
	$wR2 = 0.0734$	$wR2 = 0.1222$
Flack parameter	0.00(2)	--
Twin ratio	–	0.20(4)
Extinction coefficient	0.00067(6)	0.00061(7)
Largest diff. peak and hole	4.56 and -5.95 e/Å^3	7.24 and -7.62 e/Å^3

Single crystal intensity data were collected at room temperature by use of a four-circle diffractometer (CAD4) with graphite monochromatized Mo$K\alpha$ (71.073 pm) radiation and a scintillation counter with pulse height discrimination. Empirical absorption corrections were applied on the basis of psi-scan data.

The magnetic susceptibilities of polycrystalline pieces of $Eu_2Au_3In_4$ were measured with a SQUID magnetometer (MPMS, Quantum Design, Inc.) between 2 and 300 K with magnetic flux densities up to 5.5 T. The specific resistivities of $Eu_2Au_3In_4$ were determined on small blocks (typical dimensions $1 \times 1 \times 2$ mm^3) with a conventional four-probe technique. Cooling and heating curves measured between 4.2 and 300 K were identical within the error bars.

The 21.53 keV transition of ^{151}Eu with an activity of 130 MBq (2% of the total activity of a ^{151}Sm:EuF$_3$ source) was used for the Mössbauer spectroscopic experiments. The measurements were performed with a commercial helium

bath cryostat. The temperature of the absorber could be varied from 4.2 to 300 K and was measured with a metallic resistance thermometer with an accuracy better than ± 0.5 K. The source was kept at room temperature. The material for the Mössbauer spectroscopic measurements was the same as for the susceptibility and resistivity measurements. The sample was placed within a thin-walled PVC container at a thickness corresponding to about 10 mg Eu/cm^2.

RESULTS AND DISCUSSION

Structure Refinements

A needle shaped single crystal of $Sr_2Au_3In_4$ was isolated from a sample of the initial composition Sr:Au:In = 2:2:4, while an irregularly shaped single crystal of $Eu_2Au_3In_4$ was isolated from an annealed sample with the correct composition. Both crystals were examined by use of a Buerger camera. The precession photographs showed hexagonal lattices with Laue symmetry 6/*mmm* and no systematic extinctions. This led to the space groups $P6/mmm$, $P\bar{6}2m$, and $P\bar{6}m2$, of which the noncentrosymmetric group $P\bar{6}2m$ was found to be correct during the structure refinements. All relevant crystallographic data and experimental details for the data collections are listed in Table 1.

The starting atomic parameters were obtained from an automatic interpretation of direct methods with SHELX-86 (22) and both structures were sucessfully refined using SHELXL-97 (23) (full-matrix least-squares on F^2) with anisotropic atomic displacement parameters for all atoms. The $Sr_2Au_3In_4$ crystal had the opposite setting when compared with the original setting of the prototype $Hf_2Co_4P_3$ (18) and the crystal of the europium compound showed twinning by inversion with a twin ratio of 80:20 (see BASF in Table 1).

In order to check for the correct composition, the occupancy parameters were varied in a separate series of least-squares cycles along with the displacement parameters. Most sites were fully occupied within three standard deviations with the exception of the Au1 site for the strontium compound. The slightly elevated equivalent isotropic displacement parameter of 223(4) pm^2 as compared to 142(3) pm^2 and 118(3) pm^2 for, respectively, Au2 and Au3 indicated less electron density for this position. Subsequently this site was refined with a mixed Au/In occupancy with contraints on the positional and thermal parameters and assuming no defects on this atomic position. This refinement led to the composition $Sr_2Au_{2.85}In_{4.15}$, which can be seen as the upper limit of the indium rich side of the homogeneity range of $Sr_2Au_{3-x}In_{4+x}$. As a consequence, the analysis of the anisotropic displacement parameters of the neighboring atoms revealed a slightly larger $U_{33} = 411(39)$ of the In4 atoms on the site 1a 0,0,0. The introduction of a split position 0,0,*z* did not improve the refinement, but resulted in strong correlations. Since we also prepared $Sr_2Au_3In_4$ with the ideal composition, this ideal formula is used throughout the following discussion.

TABLE 2
Atomic Coordinates and Isotropic Displacement Parameters (pm^2) for $Sr_2Au_{2.85}In_{4.15}$ and $Eu_2Au_3In_4$

Atom	$P\bar{6}2m$	*x*	*y*	*z*	U_{eq}
		$Sr_2Au_{2.85}In_{4.15}$			
Sr1	3*g*	0.8180(2)	0	1/2	152(7)
Sr2	2*c*	1/3	2/3	0	144(11)
Sr3	3*f*	0.4507(2)	0	0	99(7)
Au1*	3*f*	0.1789(1)	0	0	173(6)
Au2	6*k*	0.68047(9)	0.50930(9)	1/2	147(3)
Au3	3*f*	0.65574(9)	0	0	124(3)
In1	3*g*	0.2807(2)	0	1/2	150(6)
In2	6*j*	0.8023(2)	0.6182(2)	0	128(4)
In3	6*k*	0.8764(1)	0.5257(1)	1/2	127(4)
In4	1*a*	0	0	0	259(13)
		$Eu_2Au_3In_4$			
Eu1	3*g*	0.8195(2)	0	1/2	146(8)
Eu2	2*c*	1/3	2/3	0	140(11)
Eu3	3*f*	0.4522(2)	0	0	113(7)
Au1	3*f*	0.1789(2)	0	0	176(7)
Au2	6*k*	0.6788(2)	0.5081(2)	1/2	132(5)
Au3	3*f*	0.6569(2)	0	0	115(5)
In1	3*g*	0.2807(3)	0	1/2	123(10)
In2	6*j*	0.8012(3)	0.6187(3)	0	116(7)
In3	6*k*	0.8762(2)	0.5265(2)	1/2	121(7)
In4	1*a*	0	0	0	176(20)

Note. U_{eq} is defined as one third of the trace of the orthogonalized U_{ij} tensor. The position Au1 in $Sr_2Au_{2.85}In_{4.15}$ is occupied by 79(2) % Au and 21(2) % In.

Final difference Fourier syntheses revealed slightly elevated, but not significant residual peaks (see Table 1). The largest residual peaks of 4.56 ($Sr_2Au_{2.85}In_{4.15}$) and 7.24 e/Å^3 ($Eu_2Au_3In_4$) were too close to a strontium (69 pm), respectively indium, position (77 pm) to be indicative of an additional atomic site. They most likely resulted from an incomplete absorption correction due to the irregular shape of the crystals investigated. The positional parameters and interatomic distances of the refinements are listed in Tables 2 and 3. Listings of the observed and calculated structure factors are available.[1]

Magnetic and Electrical Properties

The temperature dependence of the inverse magnetic susceptibility (3 T measurement) of $Eu_2Au_3In_4$ is shown in Fig. 1. Above 80 K the susceptibility obeys the Curie–Weiss

[1] Details may be obtained from: Fachinformationszentrum Karlsruhe, D-76344 Eggenstein-Leopoldshafen (Germany), by quoting the Registry No's. CSD-410724 ($Sr_2Au_{2.85}In_{4.15}$) and CSD-410725 ($Eu_2Au_3In_4$).

TABLE 3
Interatomic Distances (pm), Calculated with the Lattice Constants Taken from X-Ray Powder Data of $Sr_2Au_{2.85}In_{4.15}$ and $Eu_2Au_3In_4$

$Sr_2Au_{2.85}In_{4.15}$				$Eu_2Au_3In_4$			
Sr1:	2	Au3	334.3	Eu1:	2	Au3	332.2
	4	Au1	354.8		4	Au1	351.3
	2	In4	356.5		2	In4	352.2
	2	In1	370.4		2	In1	367.0
	4	In2	376.2		4	In2	374.6
	2	In3	381.5		2	In3	379.5
	2	Sr1	457.9		2	Eu1	454.9
	2	Sr1	473.4		2	Eu1	465.8
Sr2:	6	Au2	342.3	Eu2:	6	Au2	339.3
	3	In2	370.6		3	In2	368.3
	6	In3	379.6		6	In3	377.0
	3	Sr3	439.8		3	Eu3	435.9
	2	Sr2	457.9		2	Eu2	454.9
Sr3:	1	Au3	307.9	Eu3:	1	Au3	305.0
	4	Au2	326.6		4	Au2	323.9
	2	In2	340.1		2	In2	337.3
	2	In1	342.9		2	In1	342.0
	4	In3	347.1		4	In3	344.1
	1	Au1	408.1		1	Au1	407.2
	2	Sr2	439.8		2	Eu2	435.9
	2	Sr3	457.9		2	Eu3	454.9
Au1:	1	In4	268.7	Au1:	1	In4	266.4
	2	In1	275.3		2	In1	273.4
	2	In2	291.5		2	In2	287.9
	4	Sr1	354.8		4	Eu1	351.3
	1	Sr3	408.1		1	Eu3	407.1
Au2:	1	In3	280.8	Au2:	1	In3	277.6
	1	In3	282.6		1	In3	281.3
	2	In2	287.6		2	In2	286.5
	1	In1	290.6		1	In1	289.3
	2	Sr3	326.6		2	Eu3	323.9
	2	Sr2	342.3		2	Eu2	339.3
Au3:	2	In2	273.1	Au3:	2	In2	272.2
	4	In3	297.9		4	In3	296.1
	1	Sr3	307.9		1	Eu3	305.0
	2	Sr1	334.3		2	Eu1	332.2
In1:	2	Au1	275.3	In1:	2	Au1	273.4
	2	Au2	290.6		2	Au2	289.3
	4	In2	331.5		4	In2	327.7
	2	Sr3	342.9		2	Eu3	342.0
	2	Sr1	370.4		2	Eu1	367.0
In2:	1	Au3	273.1	In2:	1	Au3	272.2
	2	Au2	287.6		2	Au2	286.5
	1	Au1	291.5		1	Au1	287.9
	2	In3	315.5		2	In3	313.7
	2	In1	331.5		2	In1	327.7
	1	Sr3	340.1		1	Eu3	337.3
	1	Sr2	370.6		1	Eu2	368.3
	2	Sr1	376.2		2	Eu1	374.6
In3:	1	Au2	280.8	In3:	1	Au2	277.6
	1	Au2	282.6		1	Au2	281.3
	2	Au3	297.9		2	Au3	296.1
	2	In2	315.5		2	In2	313.7
	1	In3	321.5		1	In3	319.5
	2	Sr3	347.1		2	Eu3	344.1
	2	Sr2	379.6		2	Eu2	377.0
	1	Sr1	381.5		1	Eu1	379.5
In4:	3	Au1	268.7	In4:	3	Au1	266.4
	6	Sr1	356.5		6	Eu1	352.2

Note. Standard deviations are all equal or less than 0.4 pm. All distances within the first coordination sphere are listed. The position Au1 in $Sr_2Au_{2.85}In_{4.15}$ is occupied by 79% gold and 21% indium.

law; however, a slight convex curvature is observed, indicating a temperature independent contribution. We have thus fit the data above 80 K with a modified Curie–Weiss expression $\chi = \chi_0 + C/(T - \Theta)$ resulting in a paramagnetic Curie temperature (Weiss constant) of 4.0(5) K, an experimental magnetic moment of 7.88(5) μ_B/Eu, and a temperature independent contribution of $\chi_0 = 27(1) \times 10^{-9}$ m^3/mol. The experimental moment is close to the value of 7.94 μ_B for the free Eu^{2+} ion. The temperature independent contribution is of the order of magnitude of a Pauli paramagnet and most likely results from the conduction electrons of this metallic compound (see below).

At low external magnetic fields (0.01 T) antiferromagnetic ordering is detected at $T_N = 9.5(5)$ K (inset of Fig. 1). The upturn of the inverse susceptibility, however, is not very pronounced and accompanied with a broad minimum. The magnetization behavior of $Eu_2Au_3In_4$ is presented in Fig. 2. At 50 K, well above the Néel temperature, the magnetization curve is linear as expected for a paramagnetic compound. At 2 K the magnetization increases in a linear manner up to a critical field of $B = 0.5(2)$ T and then shows a stronger increase. This may be ascribed to a metamagnetic transition (antiparallel to parallel spin alignment), although the transition point (critical field) is not very sharp. At the highest obtainable field strength of $B = 5.5$ T the magnetization reached a value of 5.95(5) μ_B/Eu at 2 K, near the theoretical saturation magnetization of 7.0 μ_B/Eu. In view of the large unit cell and the three crystallographically independent europium positions, the magnetic structure of $Eu_2Au_3In_4$ is most likely very complex.

The temperature dependence of the specific resistivity of $Eu_2Au_3In_4$ is plotted in Fig. 3. The specific resistivity decreases with decreasing temperature as is typical for a metallic conductor. According to the room temperature

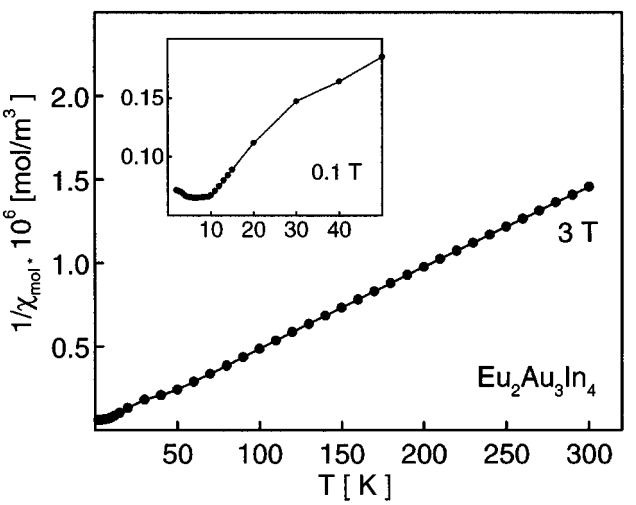

FIG. 1. Temperature dependence of the inverse magnetic susceptibility of $Eu_2Au_3In_4$ determined at an external field of $B = 3$ T. The inset shows the low temperature behavior measured at $B = 0.1$ T.

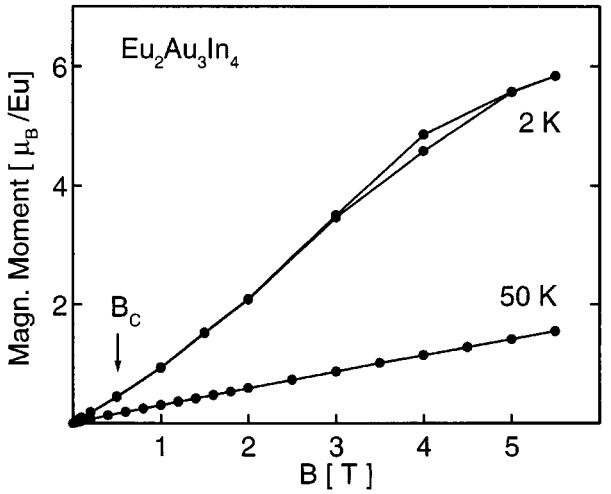

FIG. 2. Field-dependence of the magnetic moment per europium atom of $Eu_2Au_3In_4$ at 2 and 50 K.

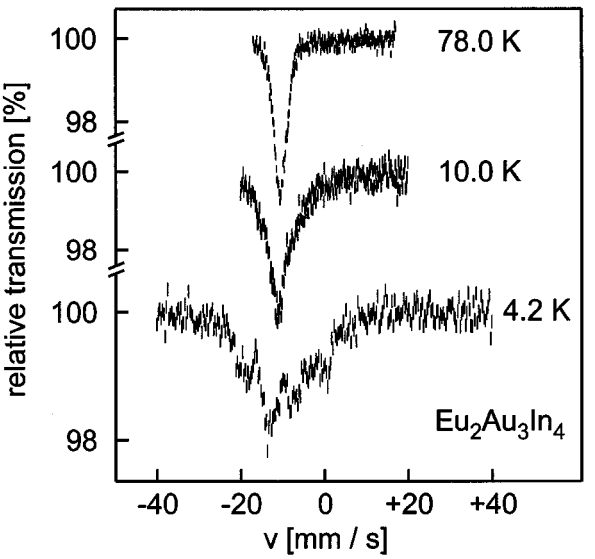

FIG. 4. Experimental ^{151}Eu Mössbauer spectra of $Eu_2Au_3In_4$ at different temperatures.

value of 75 ± 10 μΩcm, $Eu_2Au_3In_4$ is a reasonably good conductor. The large error limit accounts for the different values obtained for several samples. At low temperature, the specific resistivity has dropped to 26 μΩcm, resulting in a resistivity ratio of 0.35. No pronounced anomaly is observed below 10 K (inset of Fig. 3) where $Eu_2Au_3In_4$ orders magnetically. This is most likely due to the polycrystalline character of our sample.

^{151}*Eu Mössbauer Spectroscopy*

The ^{151}Eu Mössbauer spectra of $Eu_2Au_3In_4$ at 4.2, 10, and 78 K are presented in Fig. 4. The spectrum at 78 K shows one slightly broadened signal at an isomer shift of $\delta = -10.5(5)$ mm/s and an experimental line width of $\Gamma = 2.4(2)$ mm/s, compatible with divalent europium. It is worthwhile to note that no Eu(III) impurity was observed around $\delta = 0$ mm/s. The broadening of the Mössbauer signal most likely results from a superposition of the single signals of the three crystallographically different europium sites.

The onset of magnetic ordering in $Eu_2Au_3In_4$ is detected at 10(1) K through further broadening of the Mössbauer signal. This ordering temperature is in perfect agreement with the Néel temperature of 9.5(5) K obtained from the susceptibility measurements (Fig. 1). Complex hyperfine field splitting at the europium nuclei is detected at 4.2 K. Despite the total counting time of four days, the 4.2 K spectrum has a poor signal-to-noise ratio and therefore a poor resolution. The relative absorption was around 1% (Fig. 4) as is also the case for the 10 K spectrum. One explanation for this behavior, despite an optimized sample thickness, is certainly the strong absorption of the sample caused by the high gold content of the compound. In view of the poor signal-to-noise ratio of the spectra an assignment to the three crystallographically different europium sites was not reasonable to be carried out.

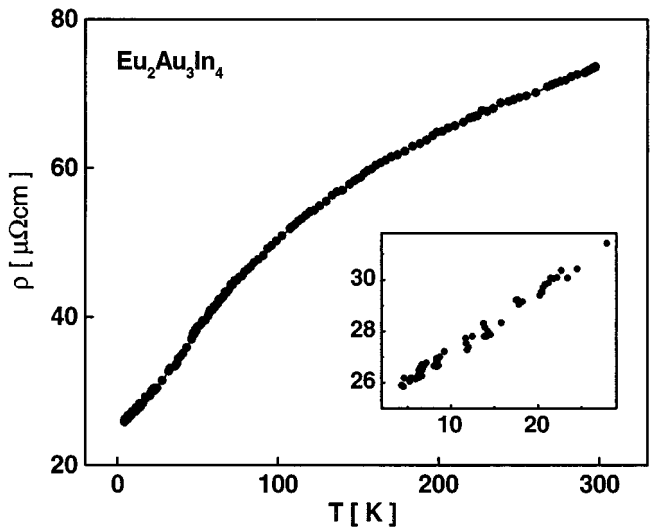

FIG. 3. Temperature dependence of the specific resistivity of $Eu_2Au_3In_4$. The low-temperature behavior is shown in the inset.

Crystal Chemistry and Chemical Bonding

New compounds $Sr_2Au_3In_4$ and $Eu_2Au_3In_4$ crystallize with the anti-$Hf_2Co_4P_3$ type (18), a structure which is typical for metal-rich phosphides. The electropositive strontium and europium atoms occupy the hafnium positions, while the indium and gold atoms occupy the cobalt, respectively

phosphorus sites. Considering Pearsons' absolute electronegativities (24) of gold (5.77 eV) and indium (3.1 eV), it is clear that the electronegative gold atoms occupy the phosphorus (5.62 eV) rather than the cobalt (4.3 eV) sites. Thus, already from this simple crystal chemical point of view, $Sr_2Au_3In_4$ and $Eu_2Au_3In_4$ may be classified as ternary aurides with at least partially negatively charged gold. This was recently also observed for the related compounds $NaAuIn_2$ (25), $Na_2Au_5In_6$ (26), and $CaAuIn_2$ (11). No Au–Au interactions are observed in the structures of $Sr_2Au_3In_4$ and $Eu_2Au_3In_4$.

The experimental molar volume of 134.6 cm^3/mol for $Sr_2Au_3In_4$ shows a reduction by about 15% when compared with the sum of the Biltz increments (27) for the neutral atoms of 158.0 cm^3/mol. This is in agreement with a charge transfer from the strontium atoms to the $[Au_3In_4]$ polyanion. Also in $CaAuIn_2$ (11) a reduction by 15% was observed. In binary aurides like CsAu (28), Rb_2Au_3 (29), or $RbAu_5$ (30) even larger volume reductions of 39, 38, 26%, respectively, are observed.

The strontium, respectively europium, atoms in $Sr_2Au_3In_4$ and $Eu_2Au_3In_4$ occupy three crystallographically different sites as outlined for the strontium compound in Fig. 5. Since the strontium and europium compound are quite similar, in the following discussion we only refer to the strontium compound. The Sr1 atoms have coordination number (CN) 20 (16 + 4) with ten indium, six gold, and four strontium neighbors. The four strontium neighbors at Sr–Sr distances of 458 and 473 pm also belong to the coordination sphere. Especially the strontium atoms with the Sr1–Sr1 distance of 473 pm complete the atomic environment (see right side of the Sr1 polyhedron in Fig. 5). The same holds true for Sr2 and Sr3. The Sr1 atoms have a sandwich-like coordination of two slightly distorted planar Au_3In_3 hexagons. Within the plane, the Sr1 atoms are coordinated to four indium and two strontium atoms. The same sandwich-like coordination with CN 20 (16 + 4) is observed for the Sr2 atoms; however, in the plane they are coordinated by three indium and three strontium atoms. The Sr3 atoms have only CN18 (13 + 5) with four strontium, eight indium, and six gold neighbors. They show a sandwich-like coordination of two distorted but planar Au_2In_3 pentagons (Fig. 5). Within the plane the Sr3 atoms are coordinated by two gold, two indium, and two strontium atoms. For this coordination polyhedron the short Sr3–Au3 distance of 308 pm is remarkable (emphasized by a solid line in Fig. 5). This distance is even smaller than the sum of Paulings' single bond radii (21) of 325 pm for strontium and gold. Similar short alkaline earth noble metal distances have recently also been observed in the ternary compounds $CaTIn_2$ (T = Pd, Pt, Au) and $SrTIn_2$ (T = Rh, Pd, Ir, Pt) with $MgCuAl_2$ type structure (11, 12). Electronic structure calculations for $CaAuIn_2$ (11) have shown that there are strong interactions between the calcium and the neighboring gold atoms. We assume that similar strong Sr–Au interactions also occur in $Sr_2Au_3In_4$.

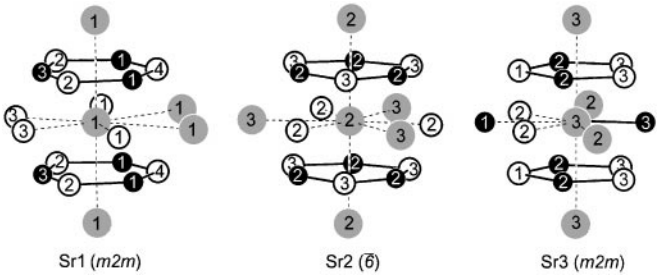

FIG. 5. Coordination polyhedra of the strontium atoms in $Sr_2Au_3In_4$. All neighbors listed in Table 3 are drawn and the site symmetries are indicated. The strontium, gold, and indium atoms are drawn as gray, black, and open circles, respectively. The sandwich-like coordinations and the strong Sr3–Au3 interactions are emphasized. The coordination polyhedra also include atoms from the second coordination sphere (for details see text).

All gold atoms have CN9 with a near-neighbor environment in the form of tricapped trigonal prisms. Both Au1 and Au2 are located in $[Sr_4In_2]$ prisms, while the Au3 atoms have a $[Sr_2In_4]$ coordination. In addition to the nine neighbors forming the tricapped trigonal prism, the Au1 atoms have one further strontium neighbor at the longer Au1–Sr3 distance of 408 pm, completing the coordination shell. Within the $Sr_2Au_3In_4$ structure we observe two different motifs of condensed trigonal prisms (face- and edge-sharing), separated by one half of the translation period c. Around the origin of the unit cell the trigonal prisms form an isolated, propeller-like column. Due to the condensation of the trigonal prisms, also the In4 atoms at the origin obtain a trigonal prismatic environment. The columns are surrounded by larger rings formed by 12 trigonal prisms which are condensed with each other. This is of course only a geometrical description; however, it is extremely useful for the comparison of related structures with similar motifs. The trigonal prismatic environment is typically observed for the phosphorus atoms in metal-rich phosphides. An overview about such crystal structures is given in Refs. (31–34).

A closer look at the interatomic distances shows that the Au–In distances range from 269 to 298 pm. Every gold atom has at least two closer indium neighbors at Au–In distances which are shorter than the sum of Paulings' single bond radii (21) of 283 pm, indicating strong covalent Au–In bonding. Short Au–In contacts have recently also been observed in the structures of GdAuIn (282 and 290 pm) (35) and $CaAuIn_2$ (282 and 285 pm) (11). Electronic structure calculations for these compounds were in agreement with strong Au–In interactions. Since the strontium, respectively europium, atoms are by far the least electronegative component of our compounds, they will largely have transferred their two valence electrons to the $[Au_3In_4]$ network. In

emphasizing the essentially covalent character of the gold–indium interactions, our compounds may be written as $[2Sr^{2+}]^{4+}[Au_3In_4]^{4-}$ and $[2Eu^{2+}]^{4+}[Au_3In_4]^{4-}$. A simple assignment of oxidation numbers for the respective atoms within the complex $[Au_3In_4]^{4-}$ polyanions is certainly difficult for these compounds. A cutout of the polyanion is presented in Fig. 6. The strontium, respectively europium, atoms fill the distorted, approximately hexagonal channels within these $[Au_3In_4]^{4-}$ polyanions.

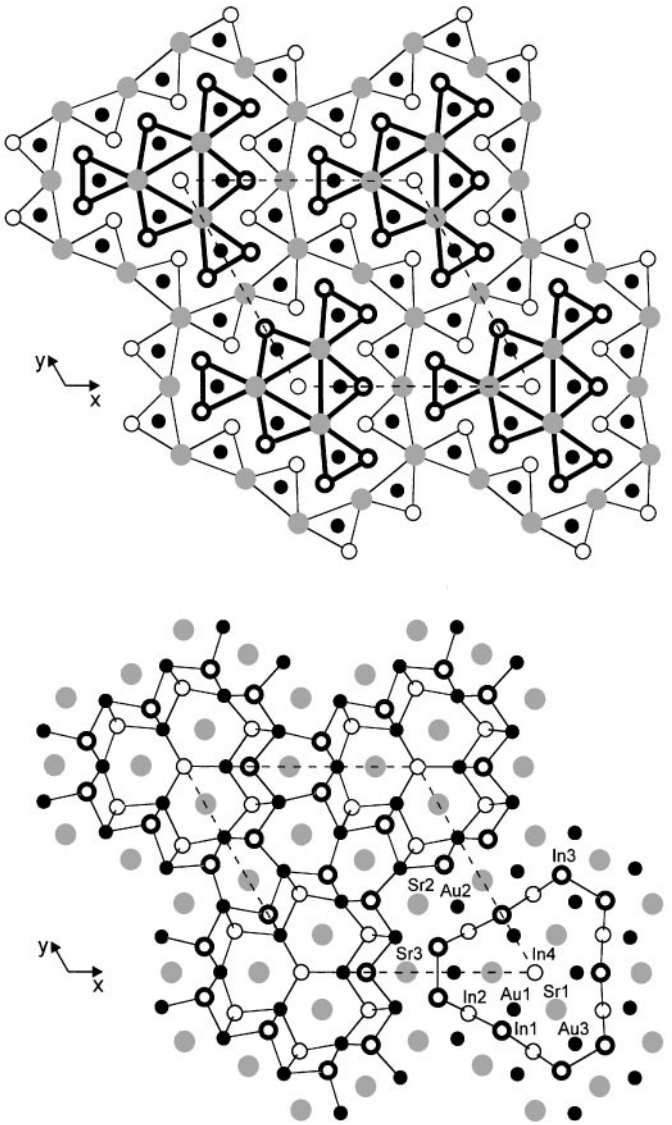

FIG. 6. Projection of the crystal structure of $Sr_2Au_3In_4$ along the c axis. All atoms lie on mirror planes at $z = 0$ and $z = 1/2$, indicated by thin and thick lines, respectively. The strontium, gold, and indium atoms are drawn as gray, black, and open circles, respectively; the atom designations are given in the lower part. In the upper drawing the trigonal prismatic environments of the gold atoms are emphasized, while the three-dimensionally infinite $[Au_3In_4]$ polyanion is outlined below, together with the one-dimensionally infinite indium cluster (see text).

As outlined in Fig. 6, the $[Au_3In_4]^{4-}$ polyanion consists of smaller slightly distorted $[In_2Au_2]$ parallelograms in which the more electronegative gold atoms have the maximum separation, avoiding Au–Au bonding. Quite similar $[In_2Au_2]$ parallelograms with a large separation of the gold atoms also occur in the TiNiSi type compounds CaAuIn (8) and EuAuIn (19).

Besides Au–In bonding In–In bonding also plays a significant role in $Sr_2Au_3In_4$. The In–In distances within the $[Au_3In_4]^{4-}$ polyanion range from 316 to 332 pm for the In1, In2, and In3 atoms, while the In4 atoms are isolated; they have only gold and strontium neighbors. The In–In contacts in $Sr_2Au_3In_4$ occur within the distorted $[In_2Au_2]$ parallelograms (Fig. 6). The In1, In2, and In3 atoms thus form a large indium cluster (indium substructure) as emphasized in the lower right hand part of Fig. 6. These indium clusters have the form of large tubes. The In–In distances in $Sr_2Au_3In_4$ have the same range as in elemental indium with a tetragonal body-centered structure ($a = 325.2$ pm, $c =$ 494.7 pm (36)). Here each indium atom has four nearest neighbors at 325.2 pm and eight further neighbors at 337.7 pm. The average In–In distance for the 12 neighbors amounts to 333.5 pm. In the Zintl phase $SrIn_2$ (37) the In–In distances are 298 pm within the puckered In_6 hexagons and 330 pm between adjacent layers. Thus, the various In–In contacts in $Sr_2Au_3In_4$ also have significant bonding character.

The composition of the two compounds $Sr_2Au_3In_4$ and $Eu_2Au_3In_4$ is not far from the $ATIn_2$ (A = Ca, Sr, Eu; T = transition metal) compounds; however, they have a distinctly different crystal chemistry. While compounds like $SrPtIn_2$, i.e., $Sr_2Pt_2In_4$, may be described as a filled $SrIn_2$ (12), $Sr_2Au_3In_4$ and $Eu_2Au_3In_4$ adopt a structure which is typical for a metal-rich phosphide. In view of this result one might expect a large variety in crystal chemistry for further alkaline earth–transition metal–indium compounds. Our recent results on $Ca_2Au_3In_4$ (38) which crystallize with a new site occupancy variant of the YCo_5P_3 type (39) already confirms this assumption.

ACKNOWLEDGMENTS

We are grateful to Prof. W. Jeitschko and Prof. H. Eckert for their interest and steady support. We are also indebted to Dipl.-Ing. U. Ch. Rodewald for the data collections on the four-circle diffractometer, to K. Wagner for the EDX measurements, and to Dr. W. Gerhartz (Degussa AG) for a generous gift of gold wire. This work was financially supported by the Fonds der Chemischen Industrie and the Deutsche Forschungsgemeinschaft (Po-573/1-2).

REFERENCES

1. P. Villars and L. D. Calvert, "Pearson's Handbook of Crystallographic Data for Intermetallic Phases," 2nd Ed. American Society for Metals, Materials Park, OH, 1991.

2. Ya. M. Kalychak, *J. Less-Common Metals* **262–263,** 341 (1997).
3. A. Szytuła and J. Leciejewicz, "Handbook of Crystal Structures and Magnetic Properties of Rare Earth Intermetallics," CRC Press, Boca Raton, FL, 1994.
4. L. V. Sysa and Ya. M. Kalychak, *Crystallogr. Rep.* **38,** 278 (1993).
5. L. V. Sysa and Ya. M. Kalychak, *Inorg. Mater.* **30,** 779 (1994).
6. L. V. Sysa, Ya. M. Kalychak, I. N. Stets', and Ya. V. Galadzhun, *Crystallogr. Rep.* **39,** 821 (1994).
7. G. Nuspl, K. Polborn, J. Evers, G. A. Landrum, and R. Hoffmann, *Inorg. Chem.* **35,** 6922 (1996).
8. D. Kußmann, R.-D. Hoffmann, and R. Pöttgen, *Z. Anorg. Allg. Chem.* **624,** 1727 (1998).
9. R.-D. Hoffmann and R. Pöttgen, submitted for publication.
10. V. I. Zaremba, O. Ya. Zakharko, Ya. M. Kalychak, and O. I. Bodak, *Dopov. Akad. Nauk Ukr. RSR, Ser. B: Geol., Khim. Biol. Nauki* 44 (1987).
11. R.-D. Hoffmann, R. Pöttgen, G. A. Landrum, R. Dronskowski, B. Künnen, and G. Kotzyba, *Z. Anorg. Allg. Chem.*, in press.
12. R.-D. Hoffmann, U. Ch. Rodewald, and R. Pöttgen, *Z. Naturforsch. B* **54,** 38 (1999).
13. L. V. Sysa, Ya. M. Kalychak, Ya. V. Galadzhun, V. I. Zaremba, L. G. Akselrud, and R. V. Skolozdra, *J. Alloys Compd.* **266,** 17 (1998).
14. Ya. M. Kalychak, Ya. V. Galadzhun, and J. Stepien-Damm, *Z. Kristallogr.* **212,** 292 (1997).
15. Ya. V. Galadzhun, R.-D. Hoffmann, R. Pöttgen, B. Künnen, and G. Kotzyba, *Eur. J. Inorg. Chem.*, in press.
16. Ya. M. Kalychak, V. M. Baranyak, V. I. Zaremba, P. Yu. Zavalii, O. V. Dmytrakh, and V. A. Bruskov, *Sov. Phys. Crystallogr.* **33,** 602 (1988).
17. R. Pöttgen, R. Müllmann, B. D. Mosel, and H. Eckert, *J. Mater. Chem.* **6,** 801 (1996).
18. E. Gangelberger, *Monatsh. Chem.* **99,** 566 (1968).
19. R. Pöttgen, *J. Mater. Chem.* **6,** 63 (1996).
20. K. Yvon, W. Jeitschko, and E. Parthé, *J. Appl. Crystallogr.* **10,** 73 (1977).
21. L. Pauling, "The Nature of the Chemical Bond and The Structures of Molecules and Crystals," Cornell University Press, Ithaca, NY, 1960.
22. G. M. Sheldrick, "SHELX-86, Program for the Solution of Crystal Structures," University of Göttingen, Germany, 1986.
23. G. M. Sheldrick, "SHELXL-97, Program for Crystal Structure Refinement," University of Göttingen, Germany, 1997.
24. R. G. Pearson, *Inorg. Chem.* **27,** 734 (1988).
25. U. Zachwieja, *Z. Anorg. Allg. Chem.* **621,** 1677 (1995).
26. U. Zachwieja, *J. Alloys Compd.* **235,** 7 (1996).
27. W. Biltz, "Raumchemie fester Stoffe," Verlag Leopold Voss, Leipzig, 1934.
28. U. Zachwieja, *Z. Anorg. Allg. Chem.* **619,** 1095 (1993).
29. U. Zachwieja, *J. Alloys Compd.* **206,** 277 (1994).
30. U. Zachwieja, *J. Alloys Compd.* **196,** 187 (1993).
31. W. Jeitschko and E. J. Reinbold, *Z. Naturforsch.* **40b,** 900 (1985).
32. W. Jeitschko, R. Brink, and P. G. Pollmeier, *Z. Naturforsch.* **48b,** 52 (1993).
33. H. G. von Schnering and W. Hönle, *in* "Encyclopedia of Inorganic Chemistry" (R. Bruce King, Ed.), p. 3106. Wiley, London, 1994.
34. Kuz'ma, Chykhrij, *in* "Handbook on the Physics and Chemistry of Rare Earths" (K. A. Gschneidner and L. Eyring, Eds.), Vol. 23, p. 285. Elsevier, Amsterdam, 1996.
35. R. Pöttgen, G. Kotzyba, E. A. Görlich, K. Łątka, and R. Dronskowski, *J. Solid State Chem.* **141,** 352 (1998).
36. J. Donohue, "The Structures of the Elements." Wiley, New York, 1974.
37. A. Iandelli, *Z. Anorg. Allg. Chem.* **330,** 221 (1964).
38. R.-D. Hoffmann and R. Pöttgen, *Z. Anorg. Allg. Chem.*, in press.
39. U. Meisen and W. Jeitschko, *J. Less-Common Metals* **102,** 127 (1984).